International Journal of Coal Geology 271 (2023) 104233

Contents lists available at ScienceDirect

International Journal of Coal Geology

journal homepage: www.elsevier.com/locate/coal

Carbon stability and morphotype composition of biochars from feedstocks in the Mekong Delta, Vietnam

H.I. Petersen [a], L. Lassen [b], A. Rudra [b], L.X. Nguyen [c], P.T.M. Do [c], H. Sanei [b,*]

[a] Geological Survey of Denmark and Greenland (GEUS), Øster Voldgade 10, 1350 Copenhagen K, Denmark
[b] Lithospheric Organic Carbon (LOC) Group, Department of Geoscience, Aarhus University, Høegh-Guldbergs Gade 2, 8000 Aarhus C, Denmark
[c] Can Tho University, College of the Environment and Natural Resources, 3/2 Street, Ninh Kieu District, Can Tho City, Viet Nam

ARTICLE INFO

Keywords:
Biochar
Temperature
Stability
Reflectance measurements
Morphotype composition
Organic petrography
Pyrolysis
Vietnam

ABSTRACT

This study investigates carbon stability of biochars produced from wood, herbaceous, and fruit agricultural waste products from southern Vietnam. The biochars were produced by pyrolysis to 500 °C, 700 °C, and 900 °C at a heating rate of 10 °C/min. Organic geochemistry and petrology have well-established measurable parameters that define degree of preservation of organic carbon in the Earth's crust. These parameters are utilized, comparatively, to infer the organic carbon stability in biochars relative to that preserved in the geological carbonaceous rocks. The stability of carbon was assessed by measuring incident-light random reflectance (%R_o) to determine the degree of thermally induced aromatization/ordering of the biochar carbon molecules. Additionally, the organic carbon content of the biochars was quantitatively separated into reactive and non-reactive carbon fractions based on thermodynamic stability of C—H and C—O bonds. The results show increasing carbon stability with increasing pyrolysis temperature and indicate high stability has been achieved at 700 °C and 900 °C where the biochars have the highest total organic carbon (TOC) contents and lowest Hydrogen Index values. Occurrence of a small quantity of readily degradable, labile free hydrocarbons (soluble organic matter; SOM) is due to condensation of the thermally generated hydrocarbons on the surfaces of the biochars. This fraction is minimized in the biochars produced at 700 °C and 900 °C due to volatilization of the free hydrocarbons at higher pyrolysis temperatures. The relatively substantial content of labile hydrocarbons associated with particulate organic matter (POM) in the 500 °C produced biochars is attributed to the incomplete pyrolyzation of the feedstock at this temperature. This fraction declines to near zero at 700 °C and 900 °C as complete carbonization is achieved at these higher temperatures. The overall carbon budget within the biochar shows that irrespective of the biochar type, over 97% of the TOC consists of highly refractory, residual carbon that geochemically is considered to possess long-term stability ("inert"). This is further underpinned by a pronounced increase in biochar mean random reflectance from <2.33% at 500 °C to >4.35% when pyrolyzed at 700 °C, indicating a highly polyaromatized condensed carbon structure. Rice husk is an exception as it yields a mean reflectance of 4.55% at 500 °C suggesting that pyrolysis temperature is not the only factor controlling %R_o and hence carbon stability. Furthermore, the biochar compositions show a relationship between feedstock and pyrolysis temperature. The biochar morphotype composition changes significantly with increasing temperature, but the analyzed biochars are all dominated by fusinoid/solid (primarily fusinoid) morphotypes with the highest initial quantity recorded at 500 °C. This quantity decreases with increasing pyrolysis temperature while porous morphotypes (tenuinetwork, crassinetwork, mixed porous, mixed dense) increase. Variations in morphotype composition observed between the biochars is attributed to the structural nature of the feedstocks.

1. Introduction

Production of biochar from the pyrolysis of agricultural biomass waste and other organic waste products is a promising technology to reduce greenhouse gas emissions by converting carbon from the dynamic biosphere pool to a stable carbon pool with long-term storage potential in the soil (biological Carbon Capture Storage, CCS) (Lehmann et al., 2021; Pulcher et al., 2022). The technique has been estimated to

* Corresponding author.
E-mail address: sanei@geo.au.dk (H. Sanei).

https://doi.org/10.1016/j.coal.2023.104233
Received 27 January 2023; Received in revised form 27 March 2023; Accepted 27 March 2023
Available online 4 April 2023

have the potential to reduce Denmark's total emission by 20–25% (Henriksen and Ahrenfeldt, 2019). Pyrolysis of biomass under anoxic or oxygen-deficient conditions is a well-known technology utilized for e.g. charcoal and biofuel production (Jahirul et al., 2012), but in recent years the use of agricultural waste products for biochar production has attracted increased focus as it has the potential to provide scalable climatic solutions. A key element for permanent storage of organic carbon in soil is the stability of carbon in biochar, i.e., its resistance against microbial degradation. Therefore, an understanding of the influence of feedstock and pyrolysis temperature on the long-term stability of biochar is critical for its use to mitigate CO_2 emissions (e.g., Crombie et al., 2013).

Many studies have shown that the biochar properties are influenced by the chemical and physical properties of their precursor feedstocks as well as the pyrolysis temperatures (e.g., Kern et al., 2012; Crombie et al., 2013; Ronsse et al., 2013; Chowdhury et al., 2016; Zhang et al., 2017). An understanding of these relationships is crucial for tailor-making biochar with long-term stability in the soil. Most experimental temperatures range from ~300 °C to 900 °C, and all studies show an increase in carbon and ash content with increasing pyrolysis temperature, while the contents of water, volatile matter, hydrogen, nitrogen, and oxygen decreases (Crombie et al., 2013; Chowdhury et al., 2016; Nguyen et al., 2018). A similar increase in carbon content and associated decrease in H/C and O/C atomic ratios with increasing temperature is observed for geological (sedimentary) organic matter undergoing thermal alteration (van Krevelen, 1993; Petersen et al., 2008; Taylor et al., 1998). For the highest pyrolysis temperatures, the carbon content of the biochar can reach or exceed ~75–80 wt% (dry basis), which is about a doubling of the carbon content in the feedstock (Kern et al., 2012; Chowdhury et al., 2016). Kern et al. (2012) showed that the 47.70 wt% (dry basis) carbon in straw increased to 75.08 wt% (dry basis) after pyrolysis in a rotary kiln at 550 °C while Chowdhury et al. (2016) demonstrated that the carbon content of 33.77 wt% in durian wood sawdust increased to 75.99 wt% after pyrolysis at 550 °C. Based on these observations, the O/C and H/C ratios have been proposed as a technique to assess biochar stability (e.g. Crombie et al., 2013; Leng et al., 2019), and specifically Spokas (2010) suggested that an O/C ratio in the range 0.2–0.6 would have an expected average residence time of 100–1000 years. However, Cross and Sohi (2013) found only a weak correlation between stable biochar carbon and the O/C ratio.

Structurally, organic carbon molecules in biochar undergo severe aromatization during the thermal carbonization process and at higher temperatures. It has been shown that at a pyrolysis temperature of 350 °C aromatic structures are formed in the biochar, and at temperatures exceeding 600 °C the biochar has attained a highly condensed aromatic structure that with further pyrolysis temperature rise attains a structure showing resemblance to graphite (Zhang et al., 2017). Ronsse et al. (2013) noted that the highest treatment temperature (HTT) is a fundamental parameter in slow pyrolysis (17 °C/min, ibid), where the pyrolysis causes devolatilization of the biomass that progressively becomes more and more condensed. Likewise, pyrolysis up to 450 °C of low rank and pure coal vitrinite showed a considerable increase in aromaticity, condensation, and stability with increasing temperature (Jiménez et al., 1999). A similar increase in aromaticity and condensation has been demonstrated for naturally coalified organic matter (Carr and Williamson, 1990; Liu et al., 2020). The structural development with increasing pyrolysis temperature has implications for the permanence of the biochar in the soil since microbial mineralization decreases with the degree of aromatization and condensation of the biochar (Bruun et al., 2008; Woolf et al., 2021).

Apart from affecting carbon stability, the pyrolysis temperature and feedstock composition also have a significant impact on the physical properties of the biochar, including quantity, porosity and specific surface area (BET) (Ronsse et al., 2013; Chowdhury et al., 2016). The changes in physical properties illustrate a dilemma between more stable, undegradable biochar produced at high pyrolysis temperatures and a higher biochar yield at lower temperatures where the biochar is less carbonized (Antal Jr. and Grønli, 2003; Bruun et al., 2009; Nguyen et al., 2018). Chowdhury et al. (2016) showed that the quantity of biochar produced at 350 °C and 550 °C decreased from ~67% to ~25%. The BET, porosity, and number of pores, including larger ones, revealed a substantial increase from 350 to 550 °C. At the highest pyrolysis temperature large pores were observed. This latter feature is comparable to those present in combustion chars collected in coal-fired power plants and perhaps related to coalescence of smaller pores due to increased carbonization of the char (Sørensen et al., 2000), which also correlate with a reduced amount of char at high temperatures. This development should also be detectable in the biochar composition towards more porous morphotypes with increasing pyrolysis temperature.

The geological coal and source rock science has a long-standing experience with organic petrography and geochemical analysis of organic material related to source material, degree of thermal transformation (which effects stability in the soil), and morphology (e.g., Taylor et al., 1998). The current study investigates biochars produced from various Vietnamese feedstocks at different pyrolysis temperatures, including agricultural waste products (rice straw, rice husk, durian, jackfruit), wood remains (bamboo, melaleuca), and water hyacinth. The aims are to (1) assess carbon stability of the biochars by determining the degree of aromatization and molecular ordering of carbon using random reflectance (%R_o) measurements and (2) measure fractions of labile and refractory organic carbon using extended slow heating (ESH®) pyrolysis. Furthermore, we aim to determine the biochar morphotype composition with increasing pyrolysis temperature by organic petrography. The goal is to provide an assessment of carbon permanence for the study biochar based on their standing in the geological organic carbon stability ranking system. Organic geochemistry and petrology have long defined a ranking system for organic carbon based on measurable parameters that define degree of preservation of organic carbon during the diagenesis, catagenesis, and metagenesis stages in the Earth's crust. Diagenesis stage encompasses all the bacterial degradations and organic carbon mineralization processes occurring at surface to shallow burial. Catagenesis and metagenesis relate to the thermal crackdown and metamorphism of organic carbon during the exposure to the burial temperature. The comparison between the organic carbon in biochars and that preserved in the geological rocks would be the key to infer the stability of carbon.

2. Feedstock samples

The feedstocks used for biochar production were collected in the Mekong Delta region of southern Vietnam and includes wood, herbaceous, and fruit agricultural waste products. The Mekong Delta accounts for about 50% of Vietnam's total agricultural waste production (vietcetera.com, 2022). The wood residues include bamboo (*Bambusa vulgaris*) and melaleuca (*Melaleuca cajuputi*), while herbaceous residues were derived from rice straw (*Oryza sativa* L.), rice husk (*O. sativa* L.), and water hyacinth (*Eichhornia crassipes*). Fruit remains were derived from jackfruit and durian peel.

The feedstocks are different in composition, which is expected to affect how the feedstocks react to pyrolysis. The melaleuca grows in coastal swamp forests and is a tree that can be up to 30 m high with a 1 m thick trunk. Bamboo is very widespread in plantations in Vietnam and produces about 7 M ton/year of waste, and the *B. vulgaris* contains around 30% lignin and > 70% cellulose (Hartono et al., 2022). The rice straw and husk remain are major agricultural waste products in the Mekong Delta. The lignin content in rice straw ranges from c. 15–20%, while the hemicellulose+cellulose content amounts to 50–70% (NL Agency, 2013). Rice husk contains about 40% cellulose and 30% lignin, and further has a high silica content of about 20% (Phonphuak and Chindaprasirt, 2015). Excess use of nitrogen and phosphorus fertilizers combined with high precipitation have led to proliferation of the invasive water hyacinth, which poses a threat to the aquatic water

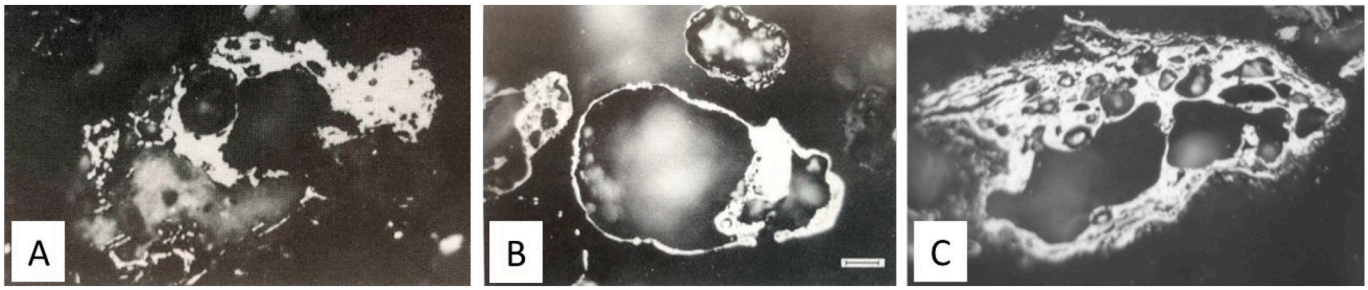

Fig. 1. Photomicrographs of charred particles of different origin but very similar morphology. (A) Natural char from Upper Jurassic rock about 160 M years old, (B) Combustion char from drop tube at 800 °C, (C) Biochar produced from rice straw pyrolysed at 500 °C.

ecosystems by forming dense floating mats that block for sunlight and effect the oxygen level (Toft et al., 2003; Nguyen et al., 2018). Compositionally water hyacinth is dominated by cellulose and hemicellulose, while it has a low lignin content of c. 4.1% (Tanpichai et al., 2019). Jackfruit and durian grow on trees and have some visual resemblance, but they are quite different rich tropical fruits with a high proportion of carbohydrates and cellulose, the latter amounting to c. 28% in jackfruit peel (Sundarraj and Ranganathan, 2017). Chemical characterization of durian peel likewise shows a dominance of cellulose and hemicellulose (57–64% and 31%, respectively) and only c. 14% lignin (Lubis et al., 2018).

3. Methods

The procedure for biochar production has been described by Nguyen et al. (2018). The feedstock biomass was dried in an oven at 105 °C, cut into 1 mm size pieces, and compressed into cylindrical particles before pyrolyzation in a Yamada Denki VMF 165 furnace. Nitrogen was initially pumped at a flow rate of 3 L/min for 30 min into the furnace to remove air followed by pyrolyzation of the feedstocks at three temperatures, 500 °C, 700 °C and 900 °C, apart from jackfruit and durian that were only pyrolyzed at 500 °C. The heating rate was for all temperatures 10 °C/min, and the maximum temperature was held for 2 h before the furnace cooled down to room temperature.

Polished blocks (pellets) suited for incident light microscopy were prepared from the 17 biochar samples according to the procedure outlined in Taylor et al. (1998). Random reflectance (%R_o) of biochar was measured using a Zeiss Axio Image 2 system equipped with Fossil-Hilgers system calibrated using a N-LASF46A standard with reference reflectance of $R_o = 1.317\%$. The %R_o measurements in each sample were carried out on 500 points (0.3 × 0.3 μm %R_o probe area) on the polished surfaces of the biochar fragments.

Table 1
Sample identification and biochar reflectance values.

Sample	ID	Feedstock	Temp.[1]	Mean[2] R_o	Std.
			°C	%	
A03380ESH	DR 500	Durian	500	1.97	0.433
A03382ESH	JF 500	Jackfruit	500	1.82	0.357
A03384ESH	WH 500	Water hyacinth	500	2.33	0.256
A03385ESH	WH 700	Water hyacinth	700	4.51	0.440
A03386ESH	WH 900	Water hyacinth	900	4.80	0.456
A03388ESH	RS 500	Rice straw	500	2.18	0.442
A03389ESH	RS 700	Rice straw	700	5.11	0.276
A03390ESH	RS 900	Rice straw	900	5.76	0.348
A03392ESH	RH 500	Rice husk	500	4.55	0.525
A03393ESH	RH 700	Rice husk	700	4.35	0.818
A03394ESH	RH 900	Rice husk	900	5.41	0.483
A03396ESH	B 500	Bamboo	500	2.21	0.288
A03397R ESH	B 700	Bamboo	700	4.67	0.562
A03398ESH	B 900	Bamboo	900	5.28	0.145
A03400ESH	M 500	Melaleuca	500	2.33	0.254
A03401ESH	M 700	Melaleuca	700	4.71	0.427
A03402R ESH	M 900	Melaleuca	900	5.58	0.201

[1] Pyrolysis temperature.
[2] Mean random reflectance.

The morphotype composition of biochar samples derived from four feedstocks (rice straw, rice husk, bamboo, and water hyacinth) at three different pyrolysis temperatures (500 °C, 700 °C, 900 °C) were determined by point counting of 400 biochar particles in each sample. Lester et al. (2018) has proposed a biomass char classification system but currently no formally established classification system for biochar is available. However biochar morphotypes are very similar to combustion chars (Fig. 1), and therefore the ICCP char classification system was used in this study (Lester et al., 2010; Hower et al., 2017; Suárez-Ruiz et al., 2017; Valentim, 2020). The basic criteria used for classification of the different morphotypes are porosity, wall thickness, internal network structure, and proportion of fused and unfused parts (for details, see Lester et al., 2010). The morphotype categories recorded are: (1) Tenuisphere and Crassisphere – spherical to angular form; (2) Tenuinetwork and Crassinetwork – internal network structure; (3) Mixed porous and Mixed dense – fused and unfused parts; (4) Inertoid and Fusinoid/solid – dense structure or inherited (original) cell structure.

A LECO CS-200 induction furnace was used to determine the content of Total Organic Carbon (TOC, wt%) in the feedstocks and the biochars. TOC was determined after removal of carbonate-bonded carbon by HCl.

TOC was also determined from Extended Slow Heating (ESH®) pyrolysis. The ESH® analysis was performed at the Lithospheric Organic Carbon laboratory (LOC), Aarhus University. The ESH® applies the automated programmed heating of 10 mg ground sample and measure the amount of thermally released hydrocarbons, CO, and CO_2. The method applies continuous pyrolysis from 100 °C to 650 °C in an inert condition (helium atmosphere). The released hydrocarbon fractions are divided based on their thermal yield pyrograms using the ESH-Slice&Dice® integration algorithm. Each hydrocarbon fraction is sliced into distinguished sections based on the temperature range and subsequently the area under each peak is integrated. The first four fractions correspond to the free hydrocarbons in the order of their thermal stability (i) light oil: 0–100 °C, (ii) mobile oil: 100–200 °C, (iii) semi-mobile oil: 200–300 °C, and (iv) immobile oil: 300–375 °C (Sanei et al., 2015; Sanei, 2019). These fractions are attributed to the free hydrocarbons, which are secondary generated from thermal crackdown of organic matter in feedstock during pyrolysis production of biochars. The hydrocarbon fractions are believed to be trapped within the biochar vacuoles and can be potentially extracted using organic solvents (soluble organic matter: SOM). The hydrocarbon fraction between 375 and 650 °C is attributed to the incompletely carbonized organic matter in feedstock at the lower end of this temperature range and thermal crackdown of the aromatic hydrocarbon biopolymers at higher temperature. This hydrocarbon fraction is believed to be insoluble in organic solvent and hence part of the particulate organic matter (POM). While all soluble hydrocarbon fractions (SOM) are regarded as labile due to existence of hydrogen as proton donor during bacterial degradation and organic mineralization, the fraction related to POM

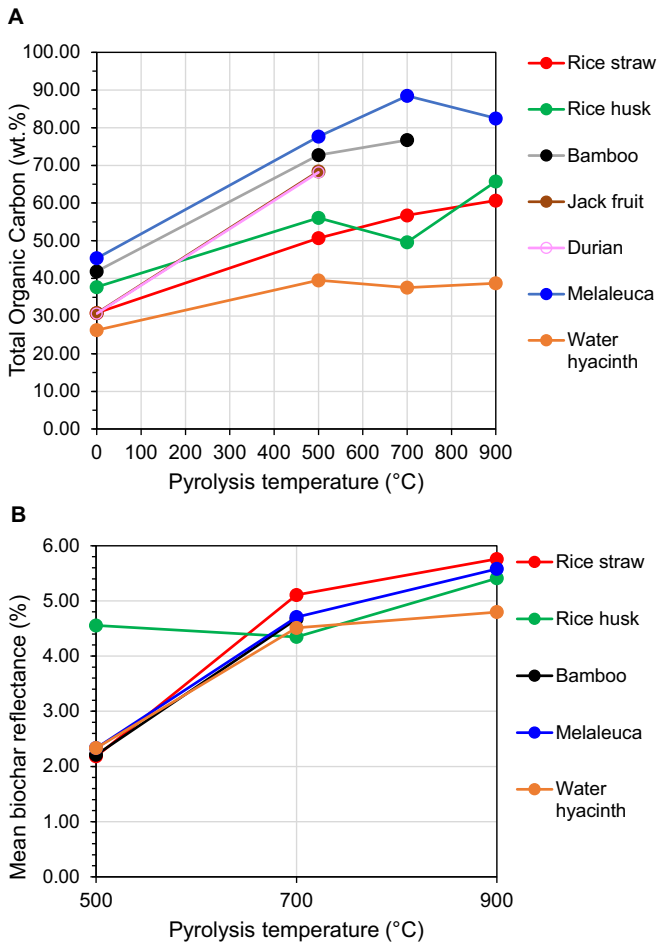

Fig. 2. A Development in total organic carbon (TOC) content with increasing pyrolysis temperature. Note that "0" refers to the non-heated feedstock. B Development in mean biochar reflectance with increasing pyrolysis temperature.

biopolymers requires more energy for degradation and hence will be selectively preserved. After completion of the pyrolysis step at 650 °C, the sample is cooled off to 100 °C and then subject of ramp heating combustion in O_2 atmosphere at the continuous heating rate of 25 °C/min until it reached 850 °C. During the oxidation stage the residual organic carbon is released and detected as CO_2 and CO after high thermal combustion. The CO and CO_2 pyrograms for all biochar samples show thermal decomposition of the residual organic carbon occurs in three major peaks attributed to three fractions of highly refractory "inert" organic carbon, in the order of their carbon stability from low to high temperature. The first fraction for all biochar samples peaks at above 300 °C and goes all the way to 700 °C. The high temperature combustion needed to breakdown the residual inert organic carbon in biochar suggests high stability of carbon in these aromatic biopolymers.

4. Results

4.1. Biochar reflectance

The mean random R_o values of the biochars pyrolyzed at 500 °C range from 1.82 to 2.33% apart from rice husk that has a R_o of 4.55% (Table 1). All biochars show a significant increase in reflectance to >4.35% when pyrolyzed at 700 °C, while the increase in %R_o is less pronounced when the pyrolysis temperature was elevated to 900 °C (Fig. 2; Table 1).

4.2. Total organic carbon (TOC)

The TOC content of all biochar samples increases with increasing temperature (Fig, 2; Table 2). Differences between the TOC contents derived from LECO and ESH® (ESH® used for calculation of GOC [generative organic carbon] and NGOC [non-generative organic carbon]) is due to different analysis methods. For most samples the difference is ≤9%, while the highest difference is recorded for the ash-rich water hyacinth biochars. However, the observed trends in TOC are the same for the two methods. The highest carbon contents close to or above 80 wt% is measured for high temperature biochars derived from the woody melaleuca and bamboo feedstocks. The durian and jack fruit biochars yield similar and high TOC contents close to 70 wt%. The biochars derived from the herbaceous water hyacinth have a relatively low TOC content just below 40 wt%, which basically does not change

Table 2
Organochemical properties and ash content of the biochars.

ID	Feedstock	Temp.[1]	TOC[2]	TOC[3]	GOC	NGOC	Reac. OC	Inert OC	Hydrogen Index	H*	N*	O*	Ash*
		°C	wt%	wt%			%	%	mg HC/g TOC	% (daf)	% (daf)	% (daf)	%
DR 500	Durian	500	68.15	74.62	1.92	72.71	3	97	12.0	n.d.	n.d.	n.d.	n.d.
JF 500	Jackfruit	500	68.42	69.87	1.04	68.83	1	99	1.6	n.d.	n.d.	n.d.	n.d.
WH 500	Water hyacinth	500	39.50	38.40	0.79	37.61	2	98	2.4	1.02	1.78	9.01	44.40
WH 700	Water hyacinth	700	37.56	41.70	0.73	40.96	2	98	0.3	0.40	1.41	6.62	51.01
WH 900	Water hyacinth	900	38.71	44.45	0.62	43.83	1	99	0.3	0.23	0.97	5.58	51.39
RS 500	Rice straw	500	50.69	52.84	1.03	51.81	2	98	5.5	n.d.	n.d.	n.d.	n.d.
RS 700	Rice straw	700	56.75	63.47	0.53	62.94	1	99	0.2	n.d.	n.d.	n.d.	n.d.
RS 900	Rice straw	900	60.68	62.24	0.37	61.86	1	99	0.2	n.d.	n.d.	n.d.	n.d.
RH 500	Rice husk	500	56.07	50.01	0.29	49.72	1	99	0.2	1.64	0.72	5.47	34.41
RH 700	Rice husk	700	49.61	47.05	0.35	46.70	1	99	0.3	0.69	0.61	1.53	38.14
RH 900	Rice husk	900	65.73	57.56	0.24	57.32	0	100	0.2	0.23	0.68	0.58	39.28
B 500	Bamboo	500	72.73	72.73	1.15	71.58	2	98	6.0	3.07	0.83	7.30	11.00
B 700	Bamboo	700	76.74	77.92	0.51	77.40	1	99	0.2	1.33	0.65	3.67	13.46
B 900	Bamboo	900	75.78	80.58	0.60	79.98	1	99	0.4	0.73	0.87	0.57	13.83
M 500	Melaleuca	500	77.66	70.50	1.41	69.10	2	98	7.4	2.52	0.36	6.62	3.09
M 700	Melaleuca	700	88.48	76.51	0.57	75.94	1	99	0.5	1.30	0.33	3.17	3.09
M 900	Melaleuca	900	82.49	85.21	0.56	84.65	1	99	0.2	0.62	0.52	1.72	3.45

GOC: generative organic carbon; NGOC: non-generative organic carbon; Reac. OC: reactive organic carbon; Inert OC: inert organic carbon.
[1] Temp.: pyrolysis temperature.
[2] TOC: total organic carbon from Leco.
[3] TOC: total organic carbon from ESH®.
* Data from Nguyen et al. (2018); daf: dry ash free.

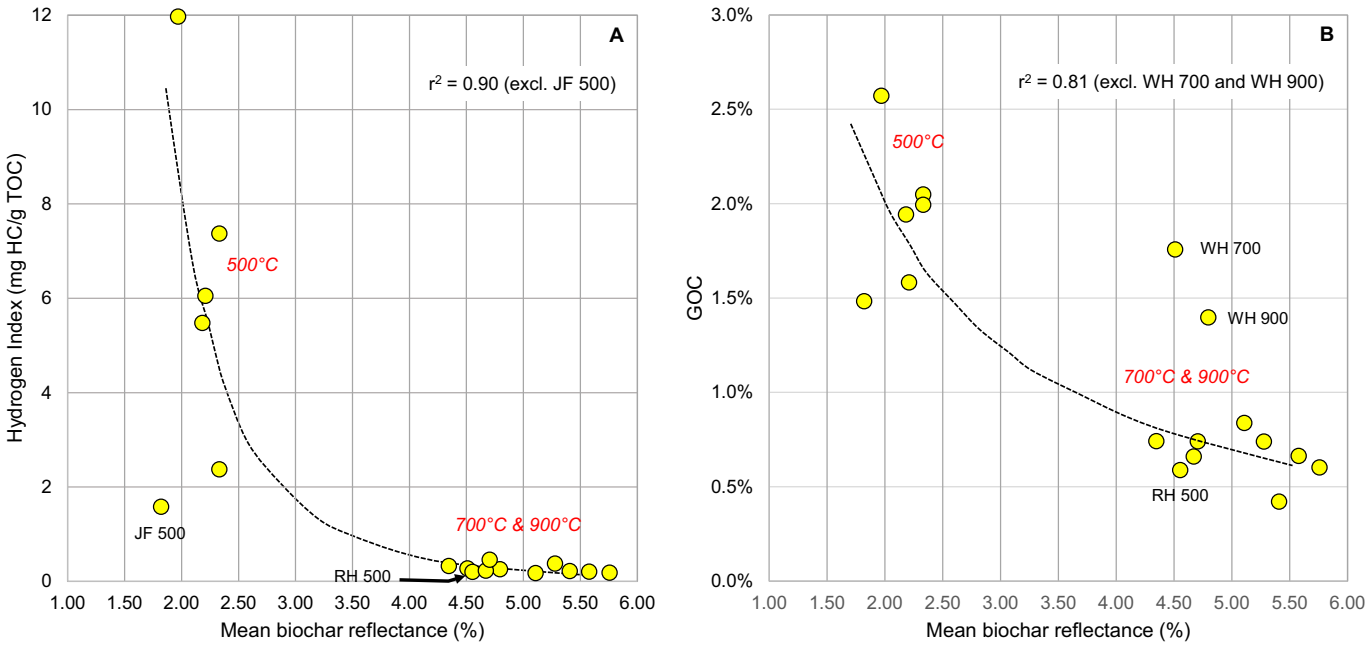

Fig. 3. A Development in the Hydrogen Index with increasing mean biochar reflectance. B Development in generative organic carbon (GOC) with increasing mean biochar reflectance.

from 500 °C to 900 °C. The biochars from rice straw and rice husk have intermediate TOC contents. Hydrogen Index (HI) values are highest for the 500 °C produced biochars but are generally very low (Fig. 3; Table 2). Most of the organic carbon is inert (non-generative, NGOC), while only a minor fraction is generative (GOC) (Fig. 3; Table 2).

4.3. Extended slow heating (ESH®)

The ESH® results show the amount of hydrocarbons distributed in the SOM and POM fractions (Fig. 4; Table 3). The SOM hydrocarbon fractions are more easily degradable compared to POM fraction as indicated by their thermal stability. The result shows that all biochars made at 500 °C (DR 500, JF 500, WH 500, RS 500, RH 500, B 500, M 500) contain considerably higher amounts of hydrocarbons compared to their counterparts made at 700 °C (WH 700, RS 700, RH 700, B 700, M 700) and 900 °C (WH 900, RS 900, RH 900, B 900, M 900) (Fig. 4; Table 3). The majority of the hydrocarbons for all samples belong to the more refractory POM fraction. However, some biochars, in particular rice straw, contain a relatively significant amount of SOM fraction. The SOM free hydrocarbon fractions are attributed to the secondary thermal cracking of the organic molecules in the feedstock and condensation on the surface of the biochars vacuoles during cooling. Organic solvents such as dichloromethane (DCM) can potentially remove the readily degradable SOM hydrocarbons from the biochars.

The inert carbon fraction is the residual organic carbon content that requires combustion between 300 and 850 °C in the presence of oxygen to break down. In contrast, the reactive carbon is the sum of all organic carbon fractions released during pyrolysis from 100 to 650 °C (CO, CO_2, and hydrocarbons). The overall carbon budget within the biochars shows that irrespective of the biochar type, over 97% of the total organic carbon in biochar consists of highly refractory, residual carbon that needs combustion beyond 300 °C. This fraction of organic carbon is by comparison to inert organic carbon in the geological record geochemically considered non-generative due to its inability to further breakdown due to diagenetic and catagenetic (burial thermal degradation) processes. Therefore, this fraction is regarded as “inert” organic carbon fraction (Fig. 5; Table 2). It is highly unlikely that low temperature shallow processes in soil and surface earth cause degradation of this fraction selectively, while other labile fractions of organic matter that require lot less energy to breakdown are always present in abundance.

4.4. Biochar composition

The composition of the rice straw, rice husk, bamboo, and water hyacinth biochars are shown in Table 4. The spherical morphotypes (tenuisphere, crassisphere; Fig. 6G) are only present in inferior quantity and will not be discussed further. The biochar compositions changes with increasing pyrolysis temperature in such a manner that some morphotypes decrease in abundance, while others increase (Table 4). All biochars independent of pyrolysis temperature are dominated by fusinoid/solid that represent inherited cellular fusinite structure or low porosity solid particles (Lester et al., 2010). The fusinoid morphotype (Figs. 6D, H; 7C, D; 8B; 9G) is much more abundant than solid (Figs. 6K, 8D) and exhibits a varying morphological appearance according to the feedstock. The quantity of fusinoid/solid decreases from 54.5 to 68.0 vol % to 32.8–43.3 vol% in the samples pyrolyzed at 500 °C and 900 °C, respectively. The porous morphotypes (tenuinetwork, crassinetwork, mixed porous, mixed dense) generally increases in quantity from 500 °C to 700 °C and/or 900 °C (Table 4), however, the feedstocks respond differently to temperature and the biochar compositions are thus distinctly different, e.g., the porous morphotypes are most abundant in the biochars derived from water hyacinth. Tenuinetwork biochars characterized by internal network structure with thin walls and high porosity is pronounced in the rice straw and water hyacinth biochars formed at 900 °C (Figs. 6A, I and 9A, C). The crassinetwork biochar, also characterized by internal network structure but lower porosity and thicker walls (Lester et al., 2010), is overall less abundant than tenuinetwork except in the rice husk biochars (Figs. 6B, C, F; 7B; 9B, D, E). Mixed porous and mixed dense biochars are likewise present in abundance in all samples but are particularly abundant in the rice husk and water hyacinth biochars formed at 700 °C and 900 °C (Figs. 6J; 7E, F, H; 8A, E–G; 9F; Table 4). The mixed biochars have fused (<75%) and unfused (>25%) parts but different porosity. It is assumed that these biochars are formed by partly devolatilization at higher temperatures of the tissue that tends to form fusinoid/solid. The biochar composition of the woody bamboo feedstock stands out by having much lower quantities of the mixed porous and dense morphotypes, while the content of inertoid is substantially higher (Fig. 8C, H; Table 4). Inertoid is a dense biochar

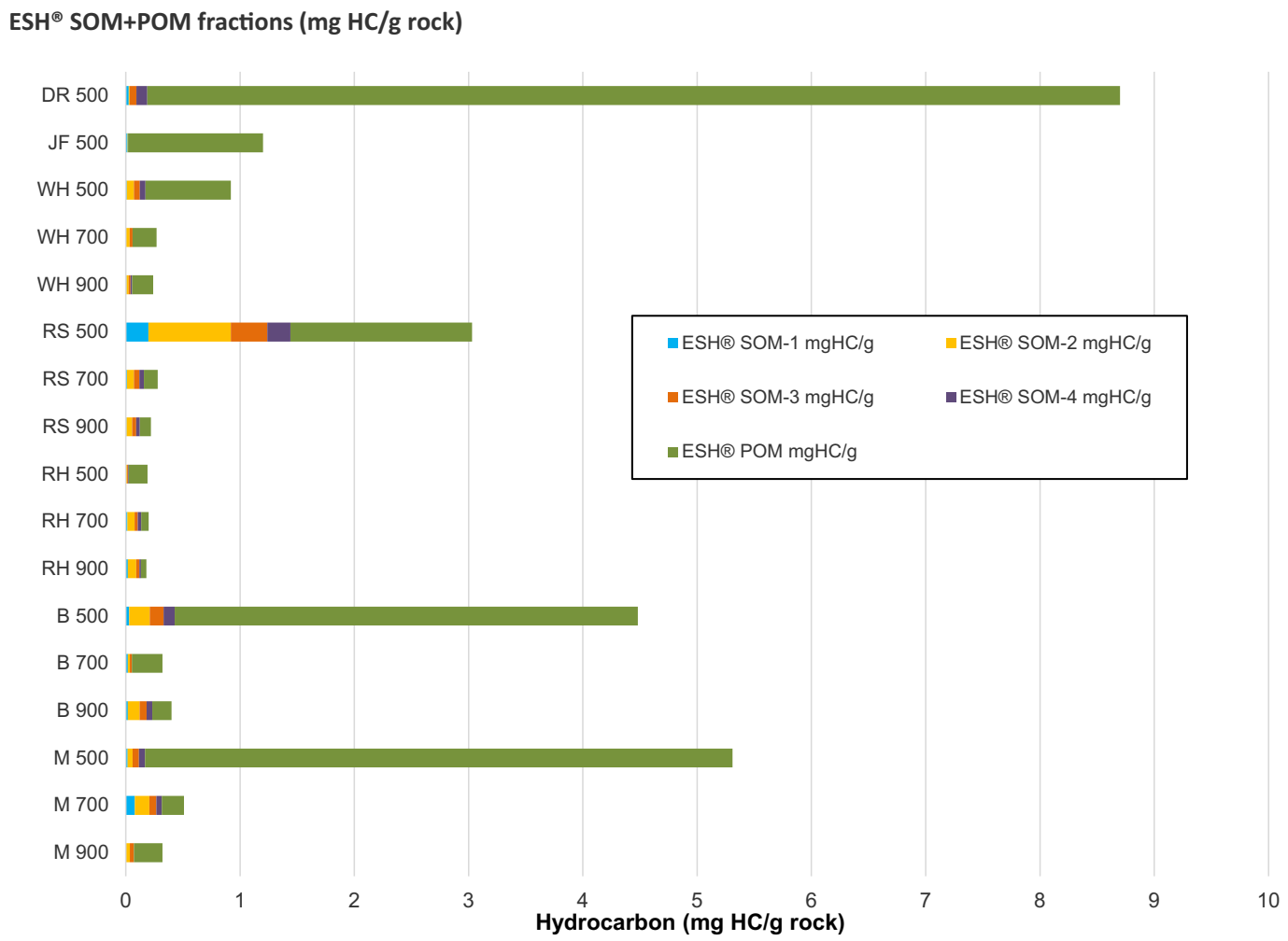

Fig. 4. The proportion of SOM and POM fractions in the biochars produced at 500 °C, 700 °C and 900 °C. Note the relatively high proportion of POM in the biochars produced at a pyrolysis temperature of 500 °C and the marked fall when the temperature is increased to 700 °C. SOM: soluble organic matter; degradable, labile free hydrocarbons. POM: particulate organic matter; likely insoluble in organic solvent. See Table 1 for sample ID.

Table 3
Soluble (SOM) and particulate (POM) organic matter in the biochars (ESH®).

ID	Feedstock	Temp.[1]	SOM-1[2]	SOM-2	SOM-3	SOM-4	Total SOM	POM[3]	S1 + S2
		°C	mg HC/g						
DR 500	Durian	500	0.03	0.01	0.06	0.09	0.19	8.51	8.70
JF 500	Jackfruit	500	0.02	0.01	0	0	0.02	1.18	1.20
WH 500	Water hyacinth	500	0.01	0.06	0.05	0.05	0.17	0.75	0.92
WH 700	Water hyacinth	700	0	0.03	0.03	0	0.06	0.21	0.27
WH 900	Water hyacinth	900	0.01	0.02	0.02	0.02	0.06	0.18	0.24
RS 500	Rice straw	500	0.20	0.72	0.32	0.20	1.44	1.59	3.03
RS 700	Rice straw	700	0.01	0.06	0.05	0.04	0.16	0.12	0.28
RS 900	Rice straw	900	0.01	0.05	0.04	0.03	0.12	0.10	0.22
RH 500	Rice husk	500	0	0.01	0.01	0.01	0.03	0.16	0.19
RH 700	Rice husk	700	0.01	0.06	0.03	0.03	0.13	0.07	0.20
RH 900	Rice husk	900	0.02	0.07	0.03	0.01	0.13	0.05	0.18
B 500	Bamboo	500	0.03	0.18	0.12	0.10	0.43	4.05	4.48
B 700	Bamboo	700	0.02	0.02	0.02	0	0.05	0.27	0.32
B 900	Bamboo	900	0.02	0.10	0.06	0.05	0.23	0.17	0.40
M 500	Melaleuca	500	0.02	0.04	0.05	0.05	0.17	5.14	5.31
M 700	Melaleuca	700	0.08	0.13	0.06	0.05	0.32	0.19	0.51
M 900	Melaleuca	900	0	0.04	0.04	0	0.07	0.25	0.32

[1] Temp.: pyrolysis temperature.
[2] SOM: soluble organic matter.
[3] POM: particulate organic matter.

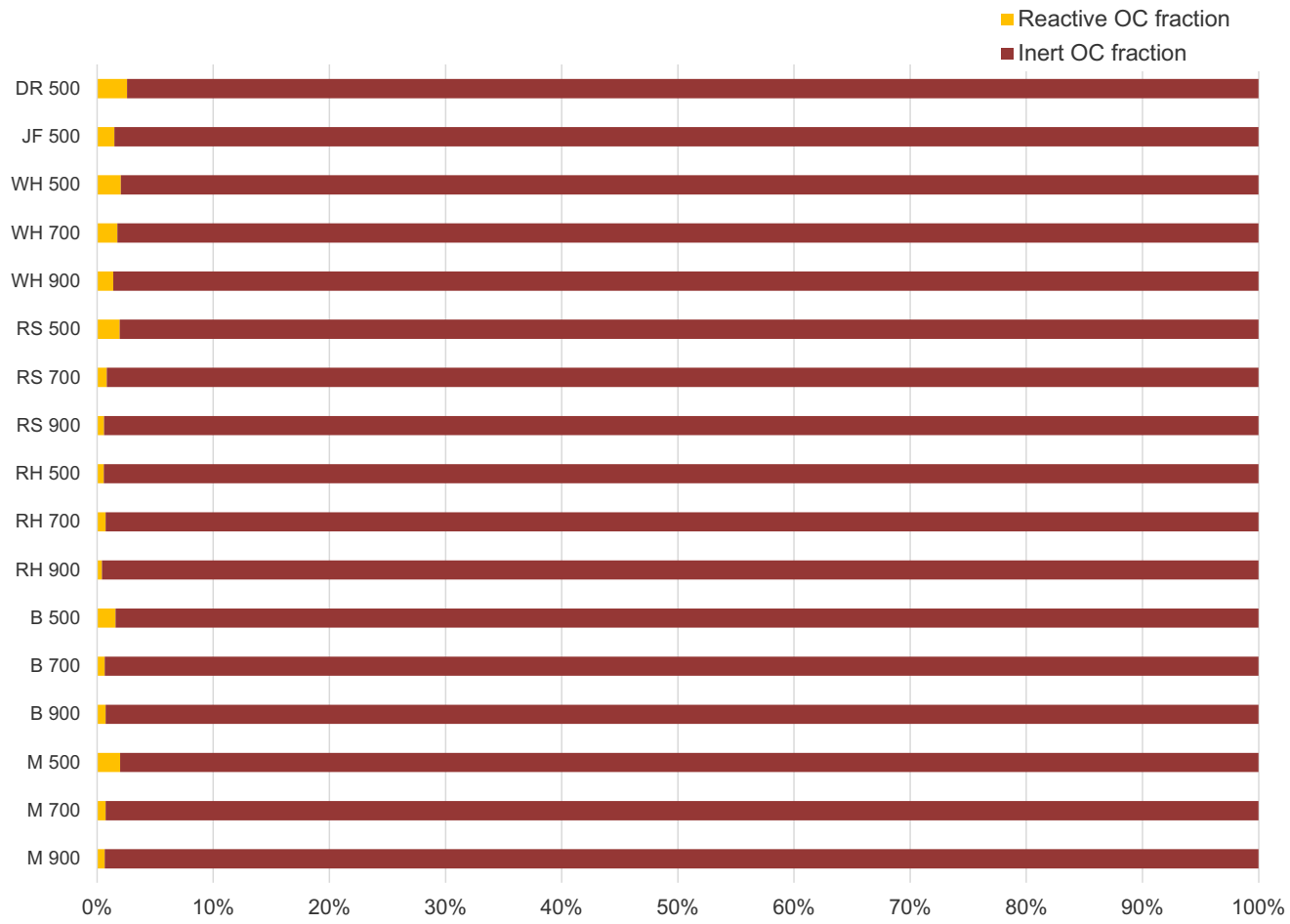

Fig. 5. The proportion of reactive and inert organic carbon fractions in the biochars produced at 500 °C, 700 °C and 900 °C. All biochars are dominated by inert organic carbon but a minor reactive fraction remains, in particular in the biochars produced at a pyrolysis temperature of 500 °C.

Table 4
Biochar composition (n = 400).

ID	Feedstock	Temp.[1]	Biochar morphotypes[2]							
			Tsph	Csph	Tnwk	Cnwk	Mx Po	Mx De	Int	Fus/So
		°C	vol%							
WH 500	Water hyacinth	500	0.3	0.5	8.3	7.8	10.3	14.3	4.3	54.5
WH 700	Water hyacinth	700	0	0.5	12.8	13.0	14.0	18.5	1.5	39.8
WH 900	Water hyacinth	900	0	0.3	19.8	12.0	15.3	18.3	1.8	32.8
RS 500	Rice straw	500	0.3	0.3	13.5	2.8	5.3	6.8	3.3	68.0
RS 700	Rice straw	700	0	1.3	11.3	3.3	6.0	14.3	2.5	61.5
RS 900	Rice straw	900	0.3	0.5	23.8	7.0	10.8	11.0	3.5	43.3
RH 500	Rice husk	500	0	0.5	4.8	11.3	5.3	16.0	3.0	59.3
RH 700	Rice husk	700	0	0	1.5	13.5	7.8	20.5	5.3	51.5
RH 900	Rice husk	900	0.3	0	4.0	8.5	12.5	31.5	0.8	42.5
B 500	Bamboo	500	0	0	0.8	4.8	1.0	10.3	18.5	65.2
B 700	Bamboo	700	0	0	13.3	9.8	2.8	5.3	26.8	42.3

[1] Temp.: pyrolysis temperature.
[2] Tsph: tenuisphere; Csph: crassisphere; Tnwk: tenuinetwork; Cnwk: crassinetwork; Mx Po: mixed porous; Mx De: mixed dense; Fus/So: fusinoid/solid

with 5–40% porosity and it can be either fused or unfused (Lester et al., 2010).

5. Discussion

5.1. Biochar stability

Biochar is a carbon-enriched pyrolysis residue that can be considered part of the heat-induced conversion of organic matter known from the geological record and coal combustion (Rosenberg et al., 1996; Petersen, 1998; Scott and Glasspool, 2007). Carbon-rich particles comparable to biochar occur naturally in geological rocks millions of years old, where they constitute mostly stable non-degradable inert particles derived from natural heat-induced transformation processes of plant remains and other organic matter (Fig. 1) (e.g., Taylor et al., 1998). This material is formally known as inertinite and natural char (International Committee for Coal and Organic Petrology (ICCP), 2001; Kwiecińska and Petersen, 2004). The pyrolysis process of biomass feedstock used to

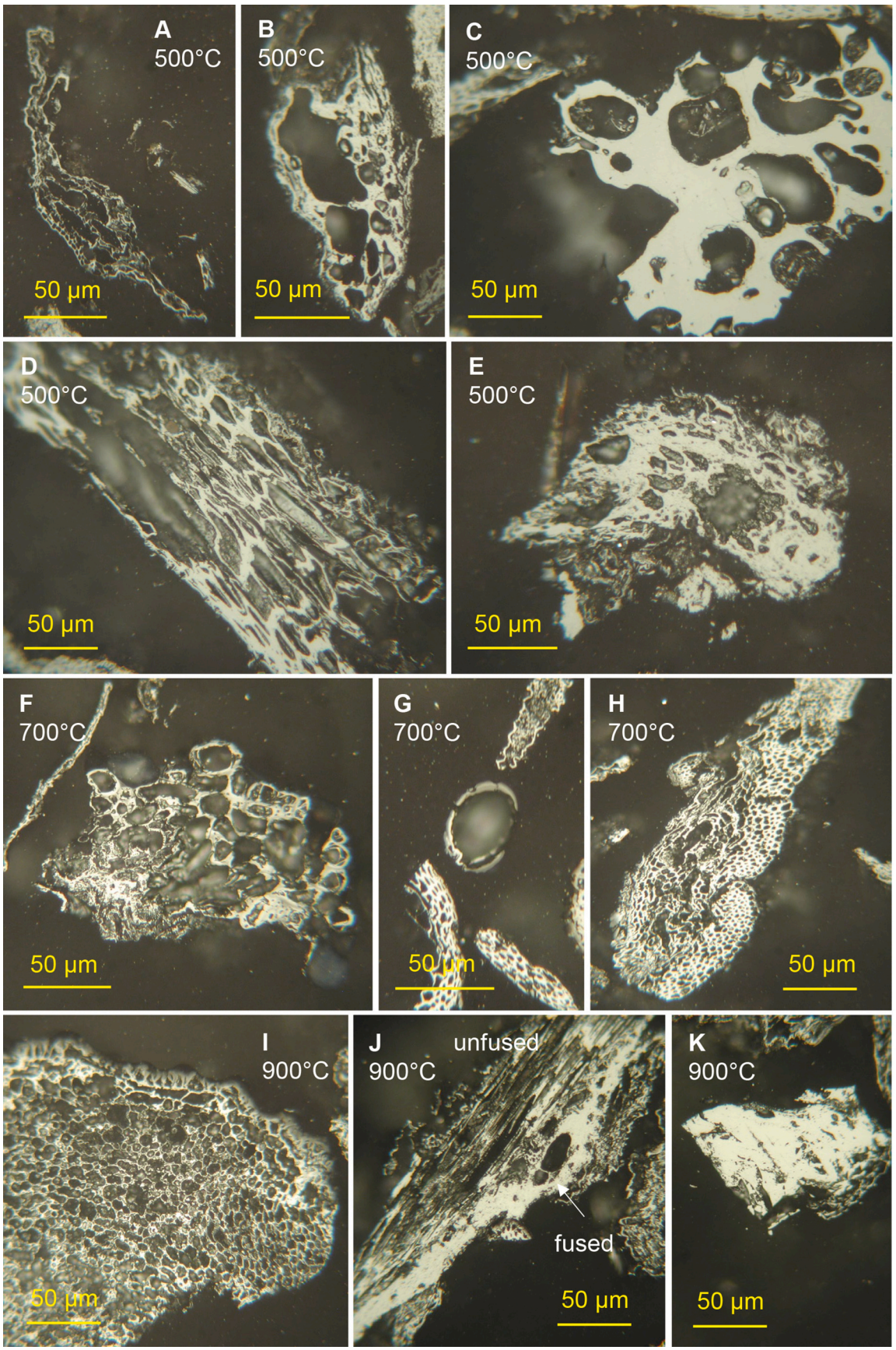

Fig. 6. Photomicrographs (reflected white light, oil immersion) of biochar morphotypes produced from rice straw by pyrolyzation at 500 °C, 700 °C and 900 °C. A Tenuinetwork, 500 °C; B-C Crassinetwork, 500 °C; D Fusinoid, 500 °C; E Inertoid, 500 °C; F Crassinetwork, 700 °C; G Crassisphere, 700 °C; H Fusinoid, 700 °C; I Tenuinetwork, 900 °C; J Mixed dense, 900 °C; K Solid, 900 °C.

produce biochar is in many aspects comparable to the natural geological thermal alteration process of organic matter induced by gradual burial into the Earth's crust apart from the process is accelerated to last only an hour or less in the laboratory. Pyrolysis of biomass constitutes likewise an alteration continuum controlled by pyrolysis temperature and feedstock type. In alignment with previous studies the current biochars show a significant increase in TOC content with increasing pyrolysis temperature (Fig. 2; Table 2; Crombie et al., 2015). The carbon enrichment with pyrolysis temperature is associated with a decrease in water, volatile matter, hydrogen, nitrogen, and oxygen contents (Table 2; Nguyen et al., 2018). The woody bamboo and melaleuca biochars produced at 700 °C have a maximum TOC content of ~77–88 wt%, while the TOC content decreases about 6 wt% in the melaleuca biochar from 900 °C pyrolysis. Durian and jack fruit were only pyrolyzed at 500 °C but shows a marked increase in TOC content comparable to bamboo (Fig. 2; Table 2). The herbaceous rice straw and husk biochars show a smaller TOC increase and maximum content. The lowest TOC content is measured in the water hyacinth biochars, which seems to have reached its maximum TOC content of ~38–39 wt% already at 500 °C (Fig. 2; Table 2). Nguyen et al. (2018) showed that the amount of produced biochar decreased with increasing pyrolysis temperature, however rice husk and water hyacinth produced higher biochar yields and considerably higher ash yields (max. 39.28% and 51.39%, respectively) than the woody bamboo and melaleuca biomasses (max. 13.83% and 3.43%, respectively). The larger quantity of relatively low-TOC biochars associated with high ash yields is well-known (e.g., Shariff et al., 2014), and is likely due to incorporation of inorganic compounds in the biochars (Domingues et al., 2017). The rice husk and water hyacinth biochars have significantly higher contents of Si and K than the other feedstocks, respectively, which is related to their growth habitat, e.g. rice husk feedstock from Japan had an ash content of 21.3% (Crombie et al., 2013; Nguyen et al., 2018).

Long-term biological carbon storage requires carbon stability of the biochar after applied in soil, and proposed half-life estimates of 100 to >1000 years have been proposed (Spokas, 2010; Wang et al., 2016). However, abundant occurrence of naturally formed chars and carbonized organic matter in geological sedimentary rocks of tens of millions of years age indicate that almost infinite stability of carbon can be achieved with sufficient thermal alteration of the organic matter (biomass). Increased structural alteration of natural thermally matured organic matter is associated with an increase in aromaticity and reflectance as suggested by Carr and Williamson (1990) and Liu et al. (2020). These authors showed that the aromatic structure changed with increasing temperature-influence from small isolated aromatic rings to polyaromatic compounds that gradually grow larger by condensation at a vitrinite reflectance (VR) of ~2.0–3.7%, with larger size polyaromatic structures developing at VR >3.7%. For coals this would correspond to the anthracite coalification stage. Laboratory experiments have also shown a clear increase in charcoal (inertinite) reflectance with increasing formation temperature (Jones et al., 1991; Jones, 1997; Scott and Glasspool, 2005). Long-term biochar permanence in the soil is related to the presence of condensed aromatic clusters (>7 fused rings) in the biochar structure, and like naturally carbonized organic matter the quantity of stable polycyclic aromatic carbon in biochar increases with pyrolysis temperature (Rombolà et al., 2016). A limit of about 75 wt% of stable polycyclic aromatic carbon has been estimated for biochars suggesting that even biochars produced at 800 °C may still contain a minor fraction of more labile carbon (Howell et al., 2022). It has been shown that at a pyrolysis temperature of 350 °C aromatic structures are formed in the biochar, and at temperatures exceeding 600 °C the biochar has attained a highly condensed aromatic structure that with further pyrolysis temperature rise attains a structure showing some resemblance with graphite (Zhang et al., 2017). Just like naturally carbonized organic matter the degree of temperature-induced transformation can be assessed by measuring the random reflectance (%R_o). The %R_o values of the biochars show a fairly similar increasing trend with increasing pyrolysis temperature, apart from rice husk that has a significantly higher %R_o at 500 °C than all other chars (Fig. 2). This indicates that pyrolysis temperature is not the only factor controlling %R_o and hence carbon stability of rice husk. In the case of rice husk biochar, composition of organic matter appears to have higher propensity to be aromatized and hence at the same pyrolysis temperature of 500 °C shows significantly higher %R_o, which is indicative of its superior carbon stability as compared to other feedstocks.

It is also notable that the biochars show a conspicuous jump in %R_o from 500 °C to 700 °C indicating a pronounced structural change towards higher aromaticity and condensation, while increasing the pyrolysis temperature from 700 °C to 900 °C has a small effect on %R_o, suggesting that the biochars already have attained sufficiently high degree of consolidation and aromatization (Fig. 2). Analogous to this a study of the relationship between reflectance and formation temperature of charcoal showed a non-linear correlation with a pronounced increase in reflectance around 500 °C (Jones et al., 1991). The sudden increase in %R_o values from 500 °C produced biochars to 700 °C produced biochars is likewise reflected in a marked decline in HI values and the proportion of generative organic carbon, although it should be stressed that none of the biochars contain more than 3% reactive organic carbon (Figs. 3 and 5; Table 2). Similarly, Crombie et al. (2015) showed that the proportion of stable carbon in biochar increased with highest treatment temperature (650 °C ibid.). Despite the fact that >97% of the measured carbon in all biochars is defined as non-generative and "inert", the 500 °C produced biochars have relatively higher quantity of labile hydrocarbons and reactive carbon relative to the 700 °C and 900 °C produced biochars, i.e. of pyrolyzable organic carbon that may be susceptive to degradation by microorganisms in the soil (Figs. 4 and 5; Table 3). The durian biochar appears to have the highest fraction of POM and reactive carbon (Figs. 4 and 5; Table 3). This suggests that incomplete carbonized biochar (too low temperature) can contain a labile organic fraction, which can account for the observed initial microbial degradation of biochar in short-term incubations and the modelled relatively short half-life times (Bruun et al., 2008; Spokas, 2010).

The woody melaleuca and bamboo feedstocks and perhaps also durian and jackfruit produced high-TOC biochars, and in addition the biochars pyrolyzed at 700 °C to 900 °C yielded R_o values >4.5% corresponding to a highly condensed, aromatized carbon structure. In a geological context the measured %R_o values correspond to anthracite to meta-anthracite coals and fusinite (char) formed by high-temperature wildfires, for example Pennsylvanian (c. 299–323 Ma) anthracite in Pennsylvania, USA, and fusinite in coal beds close to the Triassic/Jurassic boundary (c. 201 Ma), Denmark (Thomas, 2002; Petersen and Lindström, 2012). Thus, by analogy to natural formed heat-altered coaly matter this indicates almost infinite stability in the soil due to a chemical structure, which is inaccessible to microbial degradation. This indicates the high-TOC and high-%R_o biochars to have a high biological carbon sequestration potential but this should be confirmed by investigating the response of biochar subjected to abiotic oxidation in soil. Cheng et al. (2006) concluded that short-term abiotic oxidation of black carbon (BC) in soil had significance for its stability, however, it should be noted that the BC was produced from wood by combustion in a muffle furnace at only 350 °C. This is likely a too low temperature to completely alter the biomass into an inert polyaromatized structure with high permanence.

5.2. Biochar morphotype variations

As pointed out above biochars produced by pyrolysis share many chemical, structural, and thermal alteration similarities with natural-formed chars recovered from the geological record and combustion chars produced in coal-fired power plant boilers or made in the laboratory. Classification of combustion chars produced in coal-fired powerplants and in the laboratory by muffle furnace at temperatures <900 °C reveal a striking relation to coal type (feedstock) and temperature (e.g. Rosenberg et al., 1996; Sørensen et al., 2000). The char morphotype composition change significantly with increasing

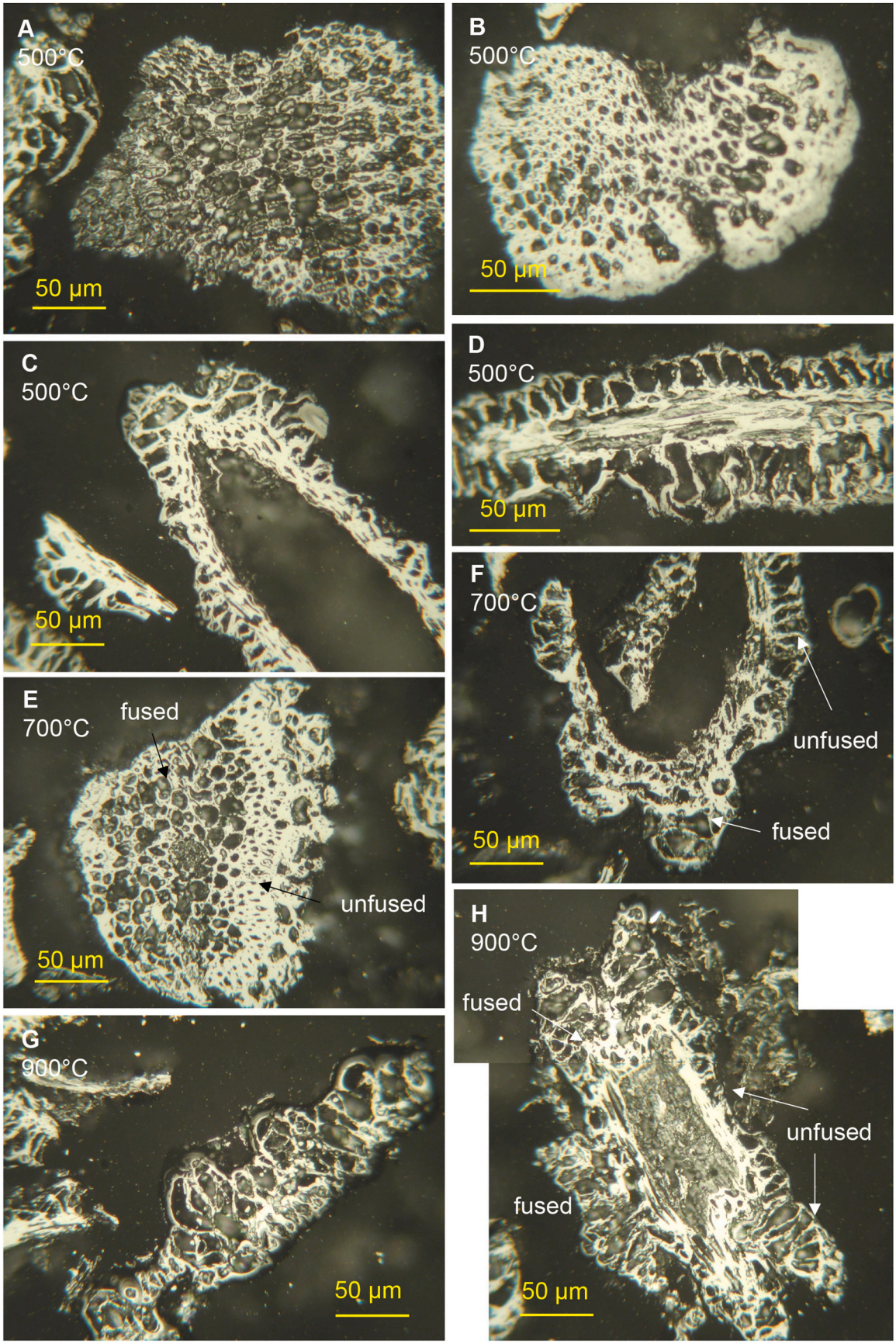

Fig. 7. Photomicrographs (reflected white light, oil immersion) of biochar morphotypes produced from rice husk by pyrolyzation at 500 °C, 700 °C and 900 °C. A Tenuinetwork, 500 °C; B Crassinetwork, 500 °C; C-D Fusinoid, 500 °C; E–F Mixed dense, 700 °C; G Tenuinetwork, 900 °C; H Mixed dense, 900 °C.

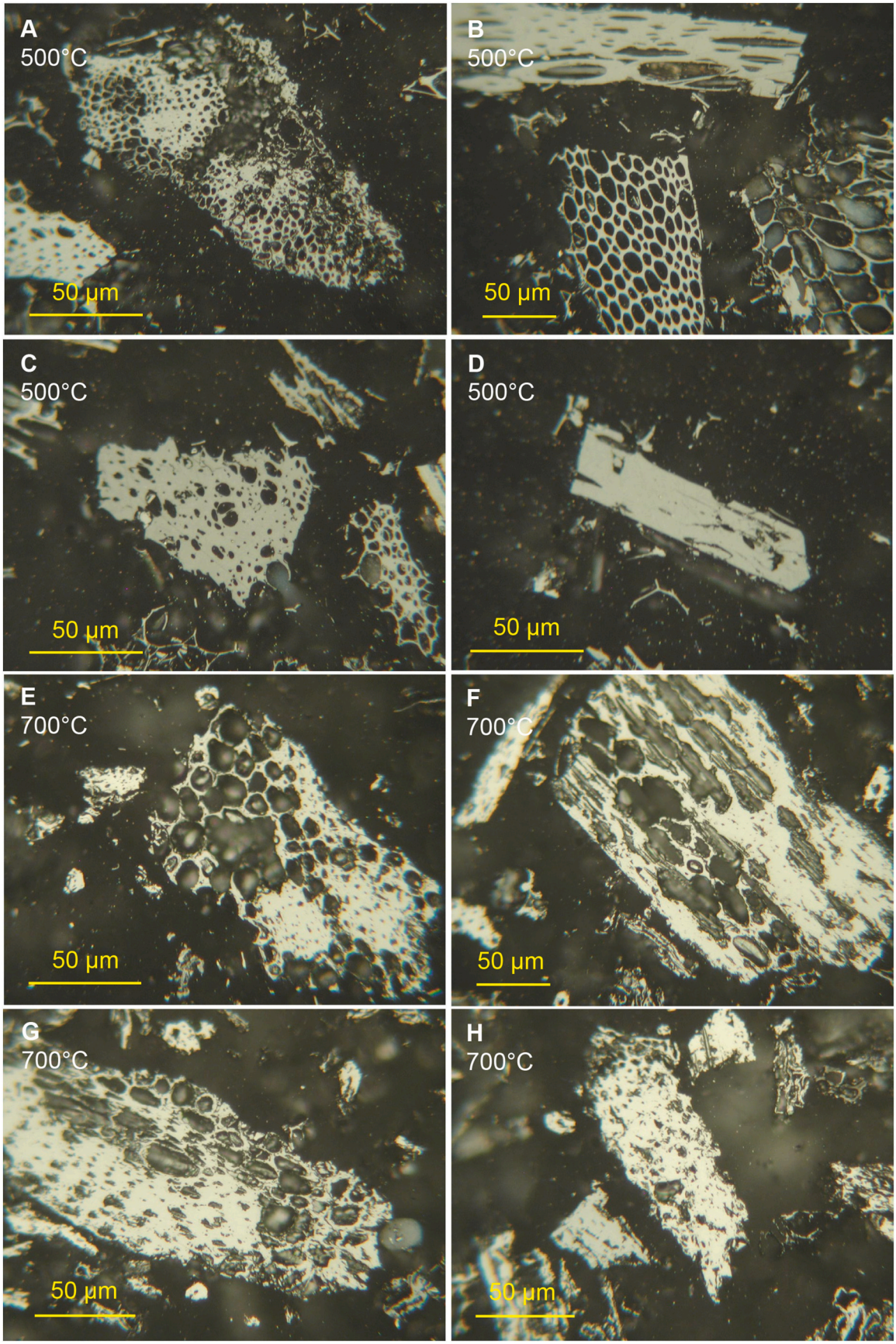

Fig. 8. Photomicrographs (reflected white light, oil immersion) of biochar morphotypes produced from bamboo by pyrolyzation at 500 °C and 700 °C. A Mixed dense, 500 °C; B Fusinoid, 500 °C; C Inertoid, 500 °C; D Solid, 500 °C; E Mixed porous, 700 °C; F–G Mixed dense, 700 °C; H Inertoid, 700 °C.

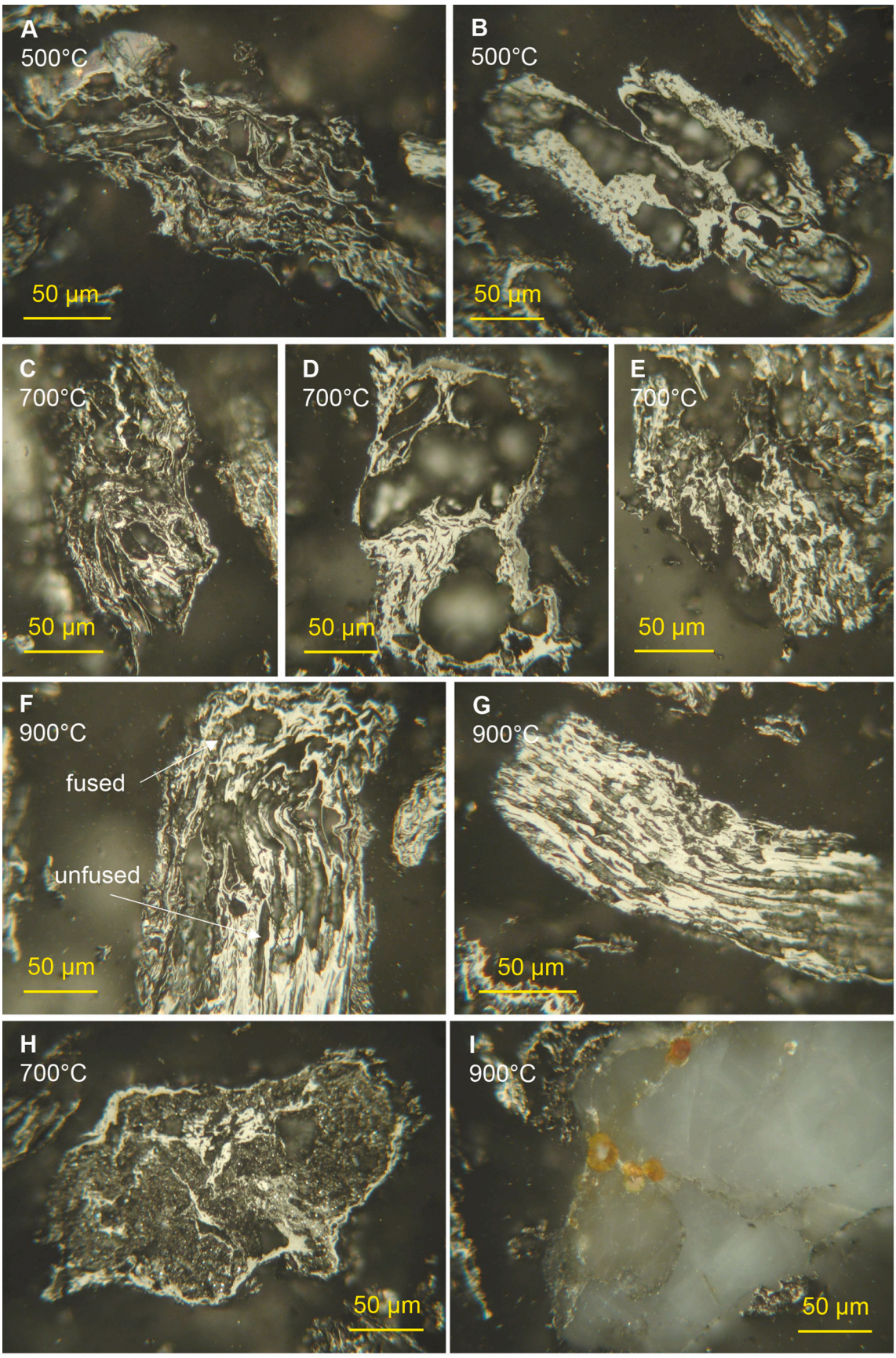

Fig. 9. Photomicrographs (reflected white light, oil immersion) of biochar morphotypes produced from water hyacinth by pyrolyzation at 500 °C, 700 °C and 900 °C. A Tenuinetwork, 500 °C; B Crassinetwork, 500 °C; C Tenuinetwork, 700 °C; D-E Crassinetwork, 700 °C; F Mixed dense, 900 °C; G Fusinoid, 900 °C; H Mineral matter filled tenuinetwork; I Mineral matter, 900 °C.

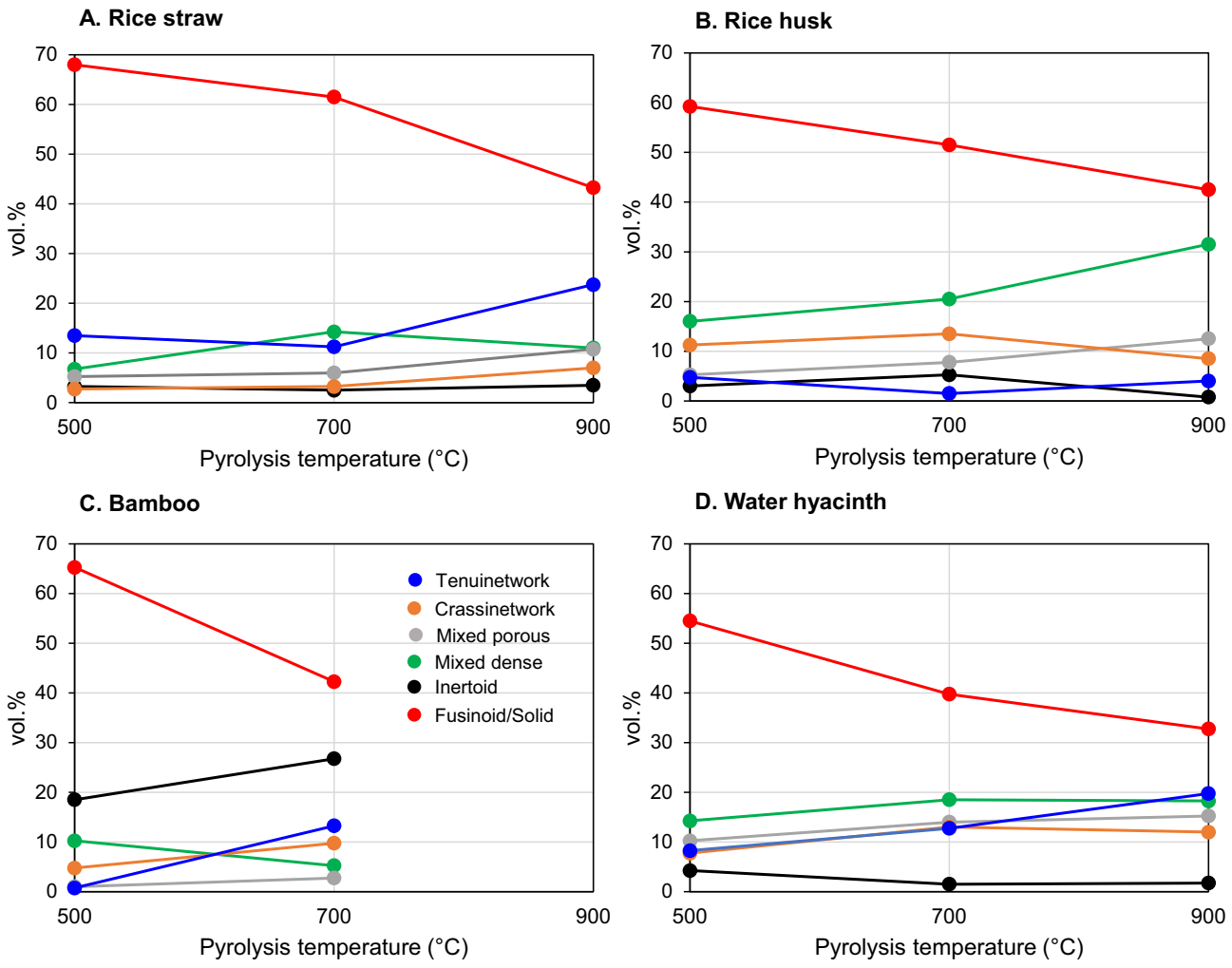

Fig. 10. Development in morphotype composition with increasing pyrolysis temperature for biochars produced from rice straw, rice husk, bamboo and water hyacinth feedstocks. The morphotype composition is dependent on both feedstock and pyrolysis temperature.

temperature. A similar development was observed for the biochars in this study (Table 4). The classified biochars show all dominance of fusinoid/solid (primarily fusinoid) morphotypes with the highest initial quantity (500 °C) in the rice straw and bamboo biochars (Figs. 6D, H, 7C, D, 8B, 9G and 10; Table 4). The high proportion of these morphotypes is likely related to the relatively low pyrolysis temperature at the absence of oxygen. The quantity of fusinoid/solid biochars decreases with increasing pyrolysis temperature in all four biochar sets due to higher reactivity of the feedstocks at elevated pyrolysis temperatures (Fig. 10; Table 4).

In the rice straw biochars the amount of porous morphotypes, in particular the high porous tenuinetwork type (Fig. 6A, I), increase at the expense of fairly dense fusinoid/solid biochars (Fig. 10). This is supported by observation of partly fused ('melted') fusinoid biochars (mixed dense, Fig. 6J). In rice husk tenuinetwork is less abundant, while the quantity of mixed dense biochars is considerably higher (Fig. 7E, F, H; Table 4). This is perhaps related to the more lignin-rich nature (30% lignin; NL Agency, 2013) of the rice husk feedstock compared to the more cellulose-rich rice straw (c. 15–20% lignin; Phonphuak and Chindaprasirt, 2015). The morphotype composition primarily changes towards a significant increase in mixed dense and partly also mixed porous with temperature increase (Fig. 10; Table 4). This again can be attributed to the increasing reactivity of the feedstock at 700 °C and 900 °C. Inertoid almost disappears at 900 °C.

The woody relatively lignin-rich bamboo produces biochars dominated by fusinoid/solid and inertoid morphotypes (Figs. 8B, C, D, H and 10; Table 4). Tenui- and crassinetwork, and inertoid biochars increase in quantity at the expense of mixed dense and fusinoid/solid biochars with increasing pyrolysis temperature (Fig. 10; Table 4). The higher proportion of porous morphotypes reflects increased reactivity of the bamboo feedstock at higher temperature, while the increase in inertoid perhaps is related to disintegration of fusinoid/solid biochars at high temperatures. However, the proportion of fusinoid/solid and inertiod biochars remains high at 700 °C, where the combined amount is 69 vol% indicating that the bamboo wood despite high temperature produces dense, relatively unfused, carbon-rich (76.7 wt%; Table 2) biochars. In combination with the high $\%R_o$ value (4.7%; Table 1) this suggests optimal long-term storage properties of the bamboo biochars.

The lignin-lean water hyacinth produces the highest proportion of porous morphotypes (tenuinetwork, crassinetwork, mixed porous, mixed dense; Fig. 9A–F), which may be related to the higher proportion of cellulose in the plant structure. The porous biochars show an increase at 700 °C, including a marked increase of tenuinetwork at 900 °C, while the fusinoid/solid biochars decline to the lowest quantity of all biochars (Fig. 10; Table 4). The biochars are often thin-walled and relatively small (broken?) suggesting considerable devolatilization during pyrolyzation, and they are commonly associated with mineral matter (Fig. 9H). Altogether the composition agrees with the substantially lower TOC content compared to the other biochars (Fig. 2; Table 2).

The biochar compositions clearly demonstrate a relationship

between feedstock and pyrolysis temperature. It is highly likely that the development in biochar morphotype composition with increasing pyrolysis temperature is associated with changing porosity and specific surface area (BET) properties, which may not have any direct influence on permanence but may be relevant for other uses of biochar such as soil amendment (e.g. water and nutrient retention in poor soils). If specific morphotype compositions can be related to desired physical properties and the biochar compositions from pyrolysis of specific feedstocks at different temperatures is known, it will be possible to tailor-make biochar for specific purposes.

6. Conclusion

Different feedstocks from the Mekong Delta region of southern Vietnam were used for biochar production at three different pyrolysis temperatures: 500 °C, 700 °C and 900 °C. The feedstocks consist of woody (bamboo, melaleuca), herbaceous (rice straw, rice husk, water hyacinth), and fruit (durian and jackfruit peel) agricultural waste products.

The results show that pyrolysis is incomplete at a temperature of 500 °C leaving behind a fraction – albeit minor – of partly degradable organic carbon. This fraction declines significantly at 700 °C and 900 °C. However, irrespective of the biochar type, over 97% of the TOC consists of highly refractory carbon that geochemically is considered to possess long-term stability indicated by: (i) high TOC contents with the woody feedstocks yielding the highest values (77–88 wt%), (ii) very low amounts of reactive organic carbon and HI values close to nil, (iii) high mean reflectance values >4.35% for the biochars produced at 700 °C and 900°, indicating a highly polyaromatized condensed carbon structure. By comparing with naturally heat-transformed organic matter the biochar data from the biochars produced at 700 °C and 900° indicate almost infinite stability in the soil, indicating a high biological carbon storage potential for high-TOC and high-%R_o biochars. This should be confirmed by investigating the response of biochar subjected to abiotic oxidation in soil.

A high %R_o of rice husk biochar produced at 500 °C suggests that pyrolysis temperature is not the only factor controlling %R_o and hence carbon stability. The composition of rice husk organic matter appears to have higher tendency to be aromatized at lower pyrolysis temperature, which is indicative of its superior carbon stability as compared to the other feedstocks.

The biochar morphotype compositions reveal that the distinct feedstocks react differently to pyrolyzation. It is also clear that the morphotype composition of each individual feedstock changes significantly with increasing pyrolysis temperature. All biochars have in common that they are dominated by fusinoid/solid (primarily fusinoid) morphotypes irrespective of pyrolysis temperature and they all show a decrease in these morphotypes with increasing pyrolysis temperature. This compositional development is accompanied by an increase in porous morphotypes (tenuinetwork, crassinetwork, mixed porous, mixed dense). The highest proportion of fusinoid/solid and inertoid morphotypes was recorded in the biochars produced from woody lignin-rich bamboo while the lignin-lean water hyacinth produces the highest proportion of porous morphotypes.

Finally the current study demonstrates the applicability of organic petrography and pyrolysis techniques to analyze biochars.

CRediT authorship contribution statement

H.I. Petersen: Conceptualization, Data curation, Formal analysis, Investigation, Methodology, Writing – original draft. **L. Lassen:** Formal analysis, Investigation, Methodology. **A. Rudra:** Formal analysis, Investigation, Methodology. **L.X. Nguyen:** Conceptualization, Formal analysis, Investigation, Methodology, Writing – review & editing. **P.T. M. Do:** Formal analysis, Investigation, Methodology. **H. Sanei:** Conceptualization, Data curation, Formal analysis, Investigation, Methodology, Writing – original draft.

Declaration of Competing Interest

The authors declare that they have no known competing financial interests or personal relationships that could have appeared to influence the work reported in this paper.

Data availability

Data has already been shared in the tables

References

Antal Jr., M.J., Grønli, M., 2003. The art, science and technology of charcoal production. Ind. Eng. Chem. Res. 42, 1619–1640.

Bruun, S., Jensen, E.S., Jensen, L.S., 2008. Microbial mineralization and assimilation of black carbon: Dependency on the degree of thermal alteration. Org. Geochem. 39, 839–845.

Bruun, S., El-Zahery, T., Jensen, L., 2009. Carbon sequestration with biochar – stability and effect on decomposition of soil organic matter. IOP Conf. Ser.: Earth Environ. Sci. 6, 242010 https://doi.org/10.1088/1755-1307/6/4/242010.

Carr, A.D., Williamson, J.D., 1990. The relationship between aromaticity, vitrinite reflectance and maceral composition of coals: implications for the use of vitrinite reflectance as a maturation parameter. Org. Geochem. 16, 313–323.

Cheng, C.-H., Lehmann, J., Thies, J.E., Burton, S.D., Engelhard, M.H., 2006. Oxidation of black carbon by biotic and abiotic processes. Org. Geochem. 17, 1477–1488.

Chowdhury, Z.Z., Karim, Md.Z., Ashraf, M.A., Khalid, K., 2016. Influence of carbonization temperature on physicochemical properties of biochar derived from slow pyrolysis of durian wood (*Durio zibethinus*) sawdust. BioResources 11, 3356–3372.

Crombie, K., Masek, O., Sohi, S.P., Brownsort, P., Cross, A., 2013. The effect of pyrolysis conditions on biochar stability as determined by three methods. GCB Bioenergy 5, 122–131.

Crombie, K., Masek, O., Cross, A., Sohi, S., 2015. Biochar – synergies and trade-offs between soil enhancing properties and C sequestration potential. GCB Bioenergy 7, 1161–1175.

Cross, A., Sohi, S.P., 2013. A method for screening the relative long-term stability of biochar. GCB Bioenergy 5, 212–220.

Domingues, R.R., Trugilho, P.F., Silva, C.A., de Melo, I.C.N.A., Melo, L.C.A., Magriotis, Z. M., Sánchez-Monedero, M.A., 2017. Properties of biochar derived from wood and high-nutrient biomasses with the aim of agronomic and environmental benefits. PLoS One 12. https://doi.org/10.1371/journal.pone.0176884.

Hartono, R., Iswanto, A.H., Priadi, T., Herawati, E., Farizky, F., Sutiawan, J., Sumardi, I., 2022. Physical, chemical, and mechanical properties of six bamboo from Sumatera Island Indonesia and its potential applications for composite materials. Polymers 14. https://doi.org/10.3390/polym14224868.

Henriksen, U.B., Ahrenfeldt, J., 2019. Reduktion af landbrugets klimaaftryk ved hjælp af pyrolyse. DTU Kemiteknik 12 (in Danish).

Howell, A., Helmkamp, S., Belmont, E., 2022. Stable polycyclic aromatic carbon (SPAC) formation in wildfire chars and engineered biochars. Sci. Total Environ. 849 https://doi.org/10.1016/j.scitotenv.2022.157610.

Hower, J.C., Groppo, J.G., Graham, U.M., Ward, C.R., Kostova, I.J., Maroto-Valer, M.M., Dai, S., 2017. Coal-derived unburned carbons in fly ash: a review. Int. J. Coal Geol. 179, 11–27.

International Committee for Coal and Organic Petrology (ICCP), 2001. The new inertinite classification (ICCP System 1994). Fuel 80, 459–471.

Jahirul, M.I., Rasul, M.G., Chowdhury, A.A., Ashwath, N., 2012. Biofuels production through biomass pyrolysis – a technological review. Energies 5, 4952–5001. https://doi.org/10.3390/en5124952.

Jiménez, A., Iglesias, M.J., Laggoun-Defarge, F., Suárez-Ruiz, I., 1999. Effect of the increase in temperature on the evolution of the physical and chemical structure of vitrinite. J. Anal. Appl. Pyrolysis 50, 117–148.

Jones, T.P., 1997. Fusain in late Jurassic sediments from the Witch Ground Graben, North Sea, U.K. Med. Nederl. Inst. Toegepaste Geow. TNO 58, 93–103.

Jones, T.P., Scott, A.C., Cope, M., 1991. Reflectance measurements and the temperature of formation of modern charcoals and implications for studies of fusain. Bull. Soc. Géol. Fr. 2, 193–200.

Kern, S., Halwachs, M., Kampichler, G., Pfeifer, C., Pröll, T., Hofbauer, H., 2012. Rotary kiln pyrolysis of straw and fermentation residues in a 3 MW pilot plant – Influence of pyrolysis temperature on pyrolysis product performance. J. Anal. Appl. Pyrolysis 97, 1–10.

Kwiecińska, B., Petersen, H.I., 2004. Graphite, semi-graphite, natural coke, and natural char classification – ICCP system. Int. J. Coal Geol. 57, 99–116.

Lehmann, J., Cowie, A., Masiello, C.A., Kammann, C., Woolf, D., Amonette, J.E., Cayuela, M.L., Camps-Arbestain, M., Whitman, T., 2021. Biochar in climate change mitigation. Nat. Geosci. 14, 883–892.

Leng, L., Huang, H., Li, H., Li, J., Zhou, W., 2019. Biochar stability assessment methods: a review. Sci. Total Environ. 647, 210–222.

Lester, E., Alvarez, D., Borrego, A.G., Valentim, B., Flores, D., Clift, D.A., Rosenberg, P., Kwiecinska, B., Barranco, R., Petersen, H.I., Mastalerz, M., Milenkova, K.S., Panaitescu, C., Marques, M.M., Thompson, A., Watts, D., Hanson, S., Predeanu, G.,

Misz, M., Tao, Wu, 2010. The procedure used to develop a coal char classification—Commission III Combustion Working Group of the International Committee for Coal and Organic Petrology. Int. J. Coal Geol. 81, 333–342.
Lester, E., Avila, C., Pang, C.H., Williams, O., Perkins, J., Gaddipatti, S., Tucker, G., Barraza, J.M., Trujillo-Uribe, M.P., Wu, T., 2018. A proposed biomass char classification system. Fuel 232, 845–854.
Liu, Y., Zhu, Y., Liu, S., Zhang, C., 2020. Evolution of aromatic clusters in vitrinite-rich coal during thermal maturation by using high-resolution transmission electron microscopy and fourier transform infrared measurements. Energy Fuel 34, 10781–10792. https://doi.org/10.1021/acs.energyfuels.0c01891.
Lubis, R., Saragih, S.W., Wirjosentono, B., Eddyanto, E., 2018. Characterization of durian rinds fiber (*Durio zubinthinus, Murr*) from North Sumatera. AIP Conf. Proc. 2049, 020069. https://doi.org/10.1063/1.5082474.
Nguyen, L.X., Do, P.T.M., Nguyen, C.H., Kose, R., Okayama, T., Pham, T.N., Nguyen, P. D., Miyanishi, T., 2018. Properties of biochars prepared from local biomass in the Mekong Delta, Vietnam. BioResources 13, 7325–7344.
NL Agency, 2013. Rice Straw and Wheat Straw. Potential Feedstocks for the Biobased Economy. NL Agency, NL Energy and Climate Change, The Netherlands, p. 31.
Petersen, H.I., 1998. Morphology, formation and palaeo-environmental implications of naturally formed char particles in coals and carbonaceous mudstones. Fuel 77, 1177–1183.
Petersen, H.I., Lindström, S., 2012. Synchronous wildfire activity rise and mire deforestation at the Triassic-Jurassic boundary. PLoS One 7. https://doi.org/10.1371/journal.pone.0047236.
Petersen, H.I., Rosenberg, P., Nytoft, H.P., 2008. Oxygen groups in coals and alginite-rich kerogen revisited. Int. J. Coal Geol. 74, 93–113.
Phonphuak, N., Chindaprasirt, P., 2015. Chapter 6: Types of waste, properties, and durability of pore-forming waste-based fired masonry bricks. In: Pacheco-Torgal, F., Lourenco, P.B., Labrincha, J.A., Kumar, S., Chindaprasirt, P. (Eds.), Eco-Efficient Mansory Bricks and Blocks. Design, Properties and Durability. Woodhead Publishing, pp. 103–127.
Pulcher, R., Balugani, E., Ventura, M., Greggio, N., Marazza, D., 2022. Inclusion of biochar in a C dynamics model based on observations from an 8-year field experiment. Soil 8, 199–211.
Rombolà, A.G., Fabbri, D., Meredith, W., Snape, C.E., Dieguez-Alonso, A., 2016. Molecular characterization of the thermally labile fraction of biochar by hydropyrolysis and pyrolysis-GC/MS. J. Anal. Appl. Pyrolysis 121, 230–239.
Ronsse, F., van Hecke, S., Dickinson, D., Prins, W., 2013. Production and characterization of slow pyrolysis biochar: influence of feedstock type and pyrolysis conditions. GCB Bioenergy 5, 105–115.
Rosenberg, P., Petersen, H.I., Thomsen, E., 1996. Combustion char morphology related to combustion temperature and coal petrography. Fuel 75, 1071–1082.
Sanei, H., 2019. A method for estimating an amount of recoverable hydrocarbons in a rock. In: Patent nr. DK180738 (PetroEval ApS, 29/1/2019).
Sanei, H., Wood, J.M., Ardakani, O.H., Clarkson, C.R., Jiang, C., 2015. Characterization of organic matter fractions in an unconventional tight gas siltstone reservoir. Int. J. Coal Geol. 150–151, 296–305.
Scott, A.C., Glasspool, I.J., 2005. Charcoal reflectance as a proxy for the emplacement temperature of pyroclastic flow deposits. Geology 33, 589–592.
Scott, A.C., Glasspool, I.J., 2007. Observations and experiments on the origin and formation of inertinite group macerals. Int. J. Coal Geol. 70, 53–66.
Shariff, A., Aziz, N.S.M., Abdullah, N., 2014. Slow pyrolysis of oil palm empty fruit bunches for biochar production and characterization. J. Phys. Sci. 25, 97–112.
Sørensen, H.S., Rosenberg, P., Petersen, H.I., Sørensen, L.H., 2000. Char porosity characterisation by scanning electron microscopy and image analysis. Fuel 79, 1379–1388.
Spokas, K.A., 2010. Review of the stability of biochar in soils: predictability of O:C molar ratios. Carbon Manag. 1, 289–303.
Suárez-Ruiz, I., Valentim, B., Borrego, A.G., Bouzinos, A., Flores, D., Kalaitzidis, S., Malinconico, M.L., Marques, M., Misz-Kennan, M., Predeanu, G., Montes, J.R., Rodrigues, S., Siavalas, G., Wagner, N., 2017. Development of a petrographic classification of fly-ash components from coal combustion and co-combustion. (an ICCP Classification System, Fly-Ash Working Group – Commission III). Int. J. Coal Geol. 183, 188–203.
Sundarraj, A.A., Ranganathan, T.V., 2017. Physicochemical characterization of jackfruit (*Artocarpus integer* (Thumb.)) peel. Research J. Pharma., Bio. Chem. Sci. 8, 2285–2295.
Tanpichai, S., Biswas, S.K., Witayakran, S., Yano, H., 2019. Water hyacinth: a sustainable lignin-poor cellulose source for the production of cellulose nanofibers. ACS Sustain. Chem. Eng. 7 (23), 18884–18893.
Taylor, G.H., Teichmüller, M., Davis, A., Diessel, C.F.K., Littke, R., Robert, P., 1998. Organic Petrology. Gebruder Borntraeger, Berlin, Stuttgart, p. 704.
Thomas, L., 2002. Coal Geology. John Wiley & Sons Ltd, Chichester, England, p. 384.
Toft, J.D., Simenstad, C.A., Cordell, J.R., Grimaldo, L.F., 2003. The effects of introduced water hyacinth on habitat structure, invertebrate assemblages, and fish diets. Estuaries 26, 746–758.
Valentim, B., 2020. Petrography of coal combustion chars: a review. Fuel 277. https://doi.org/10.1016/j.fuel.2020.118271.
van Krevelen, D.W., 1993. Coal. Typology – Physics – Chemistry – Constitution. Elsevier, Amsterdam, p. 979.
vietcetera.com, 2022. $43M Mekong Delta Biomass Power Plant Project Gets Approval. https://vietcetera.com/en/43m-mekong-delta-biomass-power-plant-project-gets-approval.
Wang, J., Xiong, Z., Kuzyakov, Y., 2016. Biochar stability in soil: meta-analysis of decomposition and priming effects. GCB Bioenergy 8, 512–523.
Woolf, D., Lehmann, J., Ogle, S., Kishimoto-Mo, A.W., McConkey, B., Baldock, J., 2021. Greenhouse gas inventory model for biochar additions to soil. Environ. Sci. Technol. 55, 14795–14805.
Zhang, H., Chen, C., Gray, E.M., Boyd, S.E., 2017. Effect of feedstock and pyrolysis temperature on properties of biochar governing end use efficacy. Biomass Bioenergy 105, 136–146.